Differentially expressed microRNAs in Huh-7 cells expressing HCV core genotypes 3a or 1b: Potential functions and downstream pathways

YU GU, YUQIAO XU, LINA JIANG, XIANGMEI CAO, FANG LIU, HANG LI, LIYING ZHANG, ZENGSHAN LI, JING LI, JING YE and QING LI

State Key Laboratory of Cancer Biology and Department of Pathology, Xijing Hospital, Fourth Military Medical University, Xi'an, P.R. China

Received February 28, 2012; Accepted April 23, 2012

DOI: 10.3892/ijmm.2012.991

Abstract. microRNA (miRNA) dysfunction is believed to play important roles in human diseases, including viral infectious diseases. Hepatitis C virus (HCV) infection promotes the development of steatosis, cirrhosis and hepatocellular carcinoma, which is genotype-specific. In order to characterize the miRNA expression profile of Huh-7 cells expressing the HCV core 3a vs. 1b, microarrays and real-time PCR were performed. Consequently, 16 miRNAs (5 miRNAs upregulated and 11 miRNAs downregulated) were found to be dysregulated. In addition, we generated the predicted and validated targets of the differentially expressed miRNAs and explored potential downstream function categories and pathways of target genes using databases of Gene Ontology (GO) and PANTHER and the database for annotation, visualization and integrated discovery (DAVID). The computational results indicated that the dysregulated miRNAs might perform the functions of cellular metabolism and cellular growth. Finally, these biological effects were preliminarily validated. This study identifies a specific miRNA expression profile in cells expressing HCV core proteins of different genotypes (genotype 3a and 1b), which may account for the variable pathophysiological manifestation associated with HCV infection.

Introduction

Hepatitis C is a world-wide contagious liver disease caused by hepatitis C virus (HCV). As estimated by WHO, some 130-170 million people are chronically infected with HCV and are at the risk of developing liver cirrhosis and cancer. More than 350,000 people die of HCV-related liver diseases each year. HCV is an enveloped, positive-sense single-stranded RNA virus and is classified into 6 genotypes and 52 subtypes present all over the world (1).

Patients infected by different HCV genotypes show respective clinical and pathogenic data (2). Insulin resistance, steatosis and progression toward fibrosis cirrhosis, and hepatocellular carcinoma establish and develop following genotype-specific mechanisms. Moreover, the genotype influences pharmacological treatment in term of dose and duration. Genotype 1 is associated with a more aggressive disease with increased insulin resistance, worst response to therapy, higher risk of cirrhosis and hepatocellular carcinoma development, while genotype 3 is associated with increased fibrosis and steatosis (3). The mechanisms by which HCV infection promotes the development of liver disease remain unclear. The direct interaction of viral proteins, particularly core proteins, and host machinery may play important roles (4).

microRNA (miRNAs) are a class of small non-coding RNA molecules that regulate gene expression through translational repression and mRNA degradation (5). miRNAs are involved in crucial physiologic and pathologic processes (6). miRNA dysfunction has been linked to the pathophysiology of human diseases, including those resulting from virus infection (7). Recently, it has been suggested that host miRNAs play critical roles in regulating HCV infection (8).

This study was undertaken to characterize the miRNA profile of Huh-7 cells expressing the HCV core 3a vs. 1b, to predict targets of verified miRNAs and to explore potential functions and downstream pathways in order to further elucidate the role of these molecules in the pathogenesis of HCV infection.

Materials and methods

Plasmid construction. The HCV core region DNA (genotypes 3a and 1b) was synthesized according to the sequnce published in NCBI (GenBank, genotype 3a: AM263171.1, genotype 1b: EU155369.2) by Beijing AuGCT DNA-SYN Biotechnology Co., Ltd. (Beijing, China). The core region DNA was cloned into the PCMV5 vector. The HA-tagged HCV core region

Correspondence to: Dr Qing Li or Dr Jing Ye, Department of Pathology, Xijing Hospital, Fourth Military Medical University, Xi'an 710032, P.R. China
E-mail: liqing@fmmu.edu.cn
E-mail: yejing@fmmu.edu.cn

Key words: microRNA, microarray, hepatitis C virus, gene ontology

Table I. Primer sequences used.

miRNA	Forward primer (5'→3')	mirBase accession no.
hsa-miR-30a*	CTTTCAGTCGGATGTTTGCAG	MIMAT0000088
hsa-miR-663	ATTAAGGCGGGGCGCCG	MIMAT0003326
hsa-miR-423-3p	AGCTCGGTCTGAGGCCC	MIMAT0001340
hsa-miR-92b	TATTGCACTCGTCCCGGC	MIMAT0003218
hsa-miR-3646	AAAATGAAATGAGCCCAGCC	MIMAT0018065
hsa-miR-3648	ATATAGCCGCGGGGATCG	MIMAT0018068
hsa-miR-16-2*	GCCAATATTACTGTGCTGCTTT	MIMAT0004518
hsa-miR-19b-1*	AGTTTTGCAGGTTTGCATCCA	MIMAT0004491
hsa-miR-224	GCAAGTCACTAGTGGTTCCGTT	MIMAT0000281
hsa-miR-629*	GTTCTCCCAACGTAAGCCCAG	MIMAT0003298
hsa-miR-32	GCTATTGCACATTACTAAGTTGC	MIMAT0000090
hsa-miR-181a-2*	ACCACTGACCGTTGACTGTACC	MIMAT0004558
hsa-miR-500a	TAATCCTTGCTACCTGGGTGAGA	MIMAT0004773
hsa-miR-542-3p	CGTGTGACAGATTGATAACTGAAA	MIMAT0003389
hsa-miR-769-5p	TGAGACCTCTGGGTTCTGAGCT	MIMAT0003886
hsa-miR-3613-3p	ACAAAAAAAAAAGCCCAACCC	MIMAT0017991
hsa-miR-146b-5p	CTGAGAACTGAATTCCATAGGCT	MIMAT0002809
hsa-let-7c	GCTGAGGTAGTAGGTTGTATGGT	MIMAT0000064
hsa-miR-132	TAACAGTCTACAGCCATGGTCG	MIMAT0000426
hsa-miR-24-1*	GTGCCTACTGAGCTGATATCAGT	MIMAT0000079
hsa-miR-455-5p	TATGTGCCTTTGGACTACATCG	MIMAT0003150
hsa-miR-192*	CTGCCAATTCCATAGGTCACA	MIMAT0004543
hsa-miR-551b	GCGACCCATACTTGGTTTCAG	MIMAT0003233
hsa-miR-664	TATTCATTTATCCCCAGCCTACA	MIMAT0005949
hsa-miR-885-5p	TCCATTACACTACCCTGCCTCT	MIMAT0004947
hsa-miR-95	TTCAACGGGTATTTATTGAGCA	MIMAT0000094
hsa-miR-34b*	TAGGCAGTGTCATTAGCTGATTG	MIMAT0000685

was cloned into the pcDNA3.1(+) vector using appropriate restriction sites. Direct sequencing of the expression vectors was carried out by AuGCT. Sequences were aligned in the NCBI BLAST server.

Cell culture and stable transfection. Human hepatoma Huh-7 cells were cultured at 37˚C in a 5% CO_2 atmosphere in Dulbecco's modified Eagle's medium (DMEM) supplemented with 10% fetal bovine serum (Hangzhou Sijiqing Biological Engineering Materials Co., Ltd., China). pcDNA3.1(+) plasmids containing the HA-tagged HCV genotype 3a or 1b core-encoding regions were transfected into Huh-7 cells with Lipofectamine 2000 (Invitrogen) as previously described (9). Briefly, cells were incubated with Opti-MEM medium (Invitrogen) under standard conditions for the first 6 h after transfection and then the medium was changed to DMEM containing 10% fetal calf serum without antibiotics. Twenty-four hours after transfection, the cells were cultured in the pressure selection medium containing 800 μg/ml G418 (Invitrogen). After 10-12 days, the neomycin-resistant cell colonies were isolated and maintained in the culture medium containing 400 μg/ml G418.

miRNA microarray profiling. Total-RNA was purified from Huh-7 cells expressing the HCV core using the miRNeasy mini kit (Qiagen, Valencia, CA, USA). The quality of the total-RNA was confirmed by the Agilent 2100 Bioanalyzer and RNA LabChip® kits (Agilent Technologies Inc., Santa Clara, CA, USA). Total-RNA (100 ng) was dephosphorylated with calf intestine alkaline phosphatase (GE Healthcare Europe GmbH), denatured with dimethyl sulfoxide, and labeled with pCp-Cy3 using T4 RNA ligase (GE Healthcare Europe GmbH). The labeled RNAs were hybridized to Agilent human miRNA microarrays for 20 h at 55˚C with rotation. After hybridization and washing, the arrays were scanned with an Agilent microarray scanner using high dynamic range settings as specified by the manufacturer. The Agilent Feature Extraction software was used to extract the data.

Real-time fluorescent reverse transcription-polymerase chain reaction for quantification of miRNAs. Quantitative stem-loop real time PCR (qRT-PCR) was carried out to detect and quantify miRNAs whose alteration was more than 3-fold between the HCV core 3a and 1b treatment groups according to the microarray profiling results. Primers for qRT-PCR were synthesized by AuGCT. All used primers were listed in Table I. A cDNA synthesis was carried out with the One Step PrimeScript® miRNA cDNA Synthesis kit (Takara, Dalian, China) according to the manufacturer's protocols. A quantita-

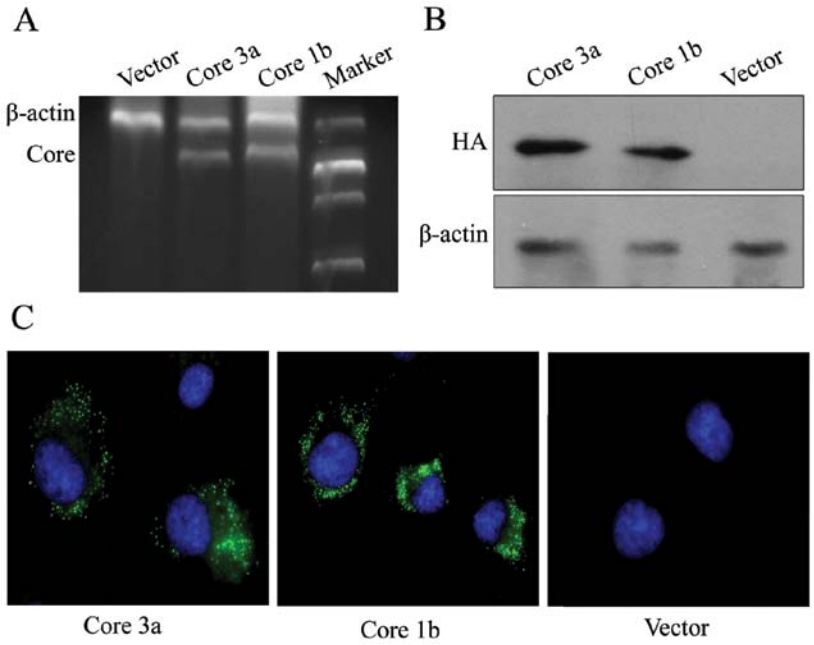

Figure 1, Efficient stable expression of HCV core protein in Huh-7 cells. (A and B) RT-PCR and western blot analyses of the mRNA and protein expression of HCV core in Huh-7 cells transfected with HCV core 3a and 1b recombinants and pcDNA3.1(+) vector. β-actin was used as control. (C) Detection of the expression of HCV core protein in Huh-7 cells by indirect immunofluorescence. The Huh-7 cells transfected with HCV core 3a and 1b recombinants and blank vector were fixed and incubated in HA monoclonal antibody to detect the core protein expression. Cell nuclei were stained by Hoechst 33258.

tive PCR was performed using SYBR® Premix Ex Taq™ II (Takara). The miRNA expression level was quantified using the Bio-Rad MyiQ™ Detection system (Bio-Rad, Hercules, CA, USA). The reactions were incubated in 96-well optical plates at 95˚C for 10 sec followed by 40 cycles of 5 sec at 95˚C and 20 sec at 60˚C. Expression analysis was performed in triplicate for each sample. The small nuclear RNA U5 was used as the normalization control.

Computational analysis of miRNA downstream target functions and pathways. We applied different computational methods to maximally analyze functions and pathways targeted by differentially expressed miRNAs. Firstly, an open access platform for miRNA database miRBase (http://www.mirbase.org) was performed to generate the targets of significantly altered miRNAs. In this webserver, we obtained the website links for validated and predicted targets while entering an miRNA accession number. For validated targets, the results from miRTarBase and TarBase were combined. For predicted targets, the microRNA.org server, PicTar and TargetScan was adopted and the predicted targets with mirSVR score ≤-0.1 was adopted in the microRNA.org server (10). Only the common target gene predicted by two different servers was listed in the final target gene table. Thereafter, the databases of GO and PANTHER were searched for functional annotation and pathway analysis. To exclude these categories identified by chance alone, the enrichment analysis was further executed using the free access program DAVID (11), where its significance was measured by the Fisher's exact test.

Immunofluorescence microscopy and dyes. Cells were fixed with 10% formaldehyde for 1 h, permeabilized with 0.01% digitonin for 30 min, and treated with 3% BSA before immunolabeling for HA. Images were obtained with an Olympus fluorescence microscope. Lipid droplets (LDs) were stained with BODIPY 493/503 (Invitrogen). Hoechst 33258 (Invitrogen) were used to stain the cell nucleus. Contrast and brightness of micrographs were adjusted by Adobe Photoshop CS for data presentation.

Lipid extraction and TAG measuring. The cell monolayer was washed with ice-cold PBS and scraped in 1 ml PBS. Lipids were extracted by the Folch method from 1-well of a 6-mutiwell dishes (12). The total lower phase was dried down, resuspended in isopropanol, and assayed with a triglyceride kit (InTec Products, Inc., Xiamen, China). Proteins were measured by a kit (Bio-Rad, Hercules, CA, USA).

Annexin V/PI staining and FCM analysis. Cells were collected for Annexin V/PI staining according to the procedures described by BD Biosciences. In brief, Huh-7 cells were washed twice with cold PBS and then resuspended in 1X binding buffer at a concentration of $1x10^6$ cells/ml. Subsequently, 100 μl of the solution was transferred into a 5 ml culture tube, and 5 μl Annexin V and 2 μl PI was added. The cells were gently mixed then incubated for 15 min at room temperature in the dark. Finally, 400 μl of 1X binding buffer was added to each tube, followed within 30 min by flow cytometry (FCM) analysis.

Statistical analysis. The Mann-Whitney U test or the Student's t-test were used to determine statistical significance by the SPSS 12.0 software.

Results

Efficient stable expression of HCV core proteins in Huh-7 cells. First, we obtained the cDNA fragments of encoding HCV different genotype core proteins and then constructed

Table II. Dysregulated miRNAs between Huh-7 cells transfected by HCV core 3a and 1b detected by microarray.

miRNAs	Fold (downregulated)	miRNAs	Fold (upregulated)
hsa-miR-224	0.31	hsa-miR-30a*	10.4
hsa-miR-629*	0.14	hsa-miR-663	8.39
hsa-miR-32	0.13	hsa-miR-423-3p	3.90
hsa-miR-181a-2*	0.13	hsa-miR-92b	3.82
hsa-miR-500a	0.12	hsa-miR-3646	3.78
hsa-miR-542-3p	0.12	hsa-miR-3648	3.74
hsa-miR-769-5p	0.10	hsa-miR-16-2*	3.66
hsa-miR-3613-3p	0.10	hsa-miR-19b-1*	3.56
hsa-miR-146b-5p	0.10		
hsa-let-7c	0.10		
hsa-miR-132	0.09		
hsa-miR-24-1*	0.09		
hsa-miR-455-5p	0.03		
hsa-miR-192*	0.02		
hsa-miR-551b	0.02		
hsa-miR-664	0.02		
hsa-miR-885-5p	0.01		
hsa-miR-95	0.01		
hsa-miR-34b*	0.01		

miRNAs presented here was >3-fold up- or downregulated.

Table III. Dysregulated miRNAs confirmed by real-time PCR.

miRNAs	Core 3a median (IQR)	Core 1b median (IQR)	Fold-change	P-value
Upregulated				
hsa-miR-30a*	0.90 (0.79, 1.01)	0.39 (0.32, 0.44)	2.34	0.004
hsa-miR-423-3p	1.57 (1.37, 1.77)	0.84 (0.72, 1.11)	1.88	0.004
hsa-miR-663	0.98 (0.94, 1.09)	0.53 (0.37, 0.60)	1.86	0.004
hsa-miR-16-2*	1.53 (1.30, 1.70)	0.84 (0.77, 0.96)	1.83	0.004
hsa-miR-92b	1.04 (0.90, 1.10)	0.61 (0.35, 0.74)	1.72	0.004
Downregulated				
hsa-miR-132	0.94 (0.85, 1.02)	1.46 (1.41, 1.63)	0.65	0.004
hsa-miR-664	1.00 (0.97, 1.04)	1.59 (1.50, 1.81)	0.63	0.004
hsa-miR-455-5p	1.07 (0.71, 1.36)	1.76 (1.63, 2.24)	0.61	0.004
hsa-miR-224	1.02 (0.96, 1.04)	2.05 (1.59, 2.59)	0.50	0.004
hsa-miR-629*	1.13 (0.58, 1.50)	2.26 (1.32, 3.90)	0.50	0.045
hsa-miR-542-3p	0.99 (0.93, 1.07)	1.96 (1.52, 2.56)	0.50	0.004
hsa-miR-34b*	0.93 (0.87, 1.21)	2.17 (1.88, 2.78)	0.43	0.004
hsa-miR-95	0.99 (0.92, 1.11)	2.34 (2.13, 2.57)	0.42	0.004
hsa-miR-192*	0.97 (0.89, 1.15)	2.62 (1.34, 4.57)	0.37	0.006
hsa-miR-885-5p	1.13 (0.98, 1.18)	3.12 (2.38, 4.08)	0.36	0.004
hsa-miR-551b	1.03 (0.86, 1.15)	3.57 (3.00, 3.93)	0.29	0.004

The relative miRNA expression level was represented by $2^{-\Delta\Delta CT}$ transformation on raw data.

HCV genotypes 3a and 1b core recombinants. Both of the recombinants were transfected into the Huh-7 cells and G418-resistant stable clones were selected and expanded under G418 selecting for 10-12 days. The total-RNA and protein were extracted from the G418-resistant clones. Different genotype core mRNA and protein expressions were identi-

Table IV. Top 15 categories of upregulated and downregulated miRNAs.

Term	Count (%)	P-value
Upregulated		
Regulation of macromolecule metabolic process	218 (31.0)	5.9E-17
Regulation of metabolic process	234 (33.2)	2.3E-16
Regulation of primary metabolic process	218 (31.0)	4.1E-16
Regulation of cellular metabolic process	224 (31.8)	1.7E-15
Regulation of biosynthetic process	198 (28.1)	1.0E-14
Regulation of cellular biosynthetic process	197 (28.0)	1.1E-14
Regulation of gene expression	192 (27.3)	1.7E-14
Regulation of macromolecule biosynthetic process	189 (26.8)	6.0E-14
Regulation of nitrogen compound metabolic process	187 (26.6)	3.4E-13
Regulation of nucleobase, nucleoside, nucleotide and nucleic acid metabolic process	185 (26.3)	5.9E-13
Regulation of transcription	172 (16.9)	3.9E-12
Biological regulation	378 (53.7)	3.1E-11
Regulation of cellular process	351 (49.9)	5.4E-11
Regulation of biological process	362 (51.4)	6.5E-11
Transcription	143 (20.3)	8.1E-11
Downregulated		
Regulation of metabolic process	386 (29.8)	4.0E-18
Regulation of cellular metabolic process	373 (28.8)	4.1E-18
Regulation of primary metabolic process	352 (27.2)	4.2E-16
Regulation of cellular biosynthetic process	323 (24.9)	4.5E-16
Regulation of macromolecule metabolic process	349 (26.9)	5.8E-16
Regulation of biosynthetic process	323 (24.9)	1.4E-15
Regulation of macromolecule biosynthetic process	311 (24.0)	1.8E-15
Regulation of gene expression	312 (24.1)	3.5E-15
Regulation of nitrogen compound metabolic process	307 (23.7)	2.7E-14
Cellular process	870 (67.2)	3.5E-14
Regulation of nucleobase, nucleoside, nucleotide and nucleic acid metabolic process	304 (23.5)	4.4E-14
Multicellular organismal development	306 (23.6)	1.6E-13
Anatomical structure development	276 (21.3)	3.3E-13
Development process	327 (25.3)	6.5E-13
Nervous system development	143 (11.0)	3.1E-12

fied by real-time PCR and western blot analyses. As shown in Fig. 1A and B, the core mRNA and protein were detected in the extracts from the Huh-7 cells transfected with HCV core 3a and 1b recombinants respectively, but not in the extract from Huh-7 cells transfected with a blank vector. Furthermore, HA-tagged 3a and 1b core proteins were also detected by indirect immunofluorescence only in Huh-7 cells stably transfected by HCV core recombinant (Fig. 1C). These results suggest that these two recombinants could express core protein effectively in the Huh-7 cells. Thus, we established independent Huh-7 cell lines that constitutively expressed core proteins of HCV genotypes 3a and 1b.

Identification of differential miRNA expression between Huh-7 cells transfected with HCV core protein of genotypes 3a and 1b. For microarray analysis, we used the commercial Agilent human miRNA (8x60K) v16 array set to examine the miRNA expression profiles of transfected Huh-7 cells with the HCV genotypes 3a and 1b core protein. miRNAs showing at least a 3-fold change in expression were considered for further investigation. In contrast to genotype 1b, there were 8 miRNAs upregulated and 19 miRNAs downregulated in Huh-7 cells stably expressing the core of the genotype 3a (Table II). To confirm the microarray results, qRT-PCR was performed on the above 27 miRNAs. U5 was used as control. The primers for the miRNAs are listed in Table I. After statistical analysis, 5 miRNAs (miR-16-2*, miR-423-3p, miR-30a*, miR-663 and miR-92b) and 11 miRNAs (miR-224, miR-629*, miR-542-3p, miR-132, miR-455-5p, hsa-miR-192*, miR-34b*, miR-95, miR-885-5p and miR-664) were determined to be respectively upregulated and downregulated (Table III).

miRNA target genes and their pathways predicted by computer-aided algorithms. The analysis of miRNA target genes and

Table V. PANTHER pathways of upregulated and downregulated miRNAs.

Term	Count (%)	P-value
Upregulated		
P00052: TGF-β signaling pathway	17 (2.4)	5.8E-3
P00059: p53 pathway	14 (2.0)	9.5E-3
P00034: integrin signaling pathway	20 (2.8)	2.0E-2
P00037: ionotropic glutamate receptor pathway	8 (1.1)	2.6E-2
Downregulated		
P00005: angiogenesis	37 (2.9)	5.2E-4
P00052: TGF-β signaling pathway	25 (1.9)	7.1E-3
P00048: PI3 kinase pathway	19 (1.5)	1.9E-2
P04398: p53 pathway feedback loops 2	12 (0.9)	2.7E-2
P00059: p53 pathway	19 (1.5)	2.8E-2
P05916: opioid prodynorphin pathway	8 (0.6)	3.0E-2
P00033: insulin/IGF pathway-protein kinase B signaling cascade	15 (1.2)	3.2E-2
P00036: interleukin signaling pathway	29 (0.7)	3.5E-2
P00016: cytoskeletal regulation by Rho GTPase	17 (1.3)	4.5E-2
P00040: metabotropic glutamate receptor group II pathway	10 (0.8)	5.0E-2
P00032: insulin/IGF pathway-mitogen activated protein kinase kinase/MAP kinase cascade	9 (0.7)	6.8E-2
P00034: integrin signaling pathway	28 (2.2)	7.9E-2
P05917: opioid proopiomelanocortin pathway	7 (0.5)	9.3E-2

Common pathways involved in both upregulated and downregulated miRNAs are underlined.

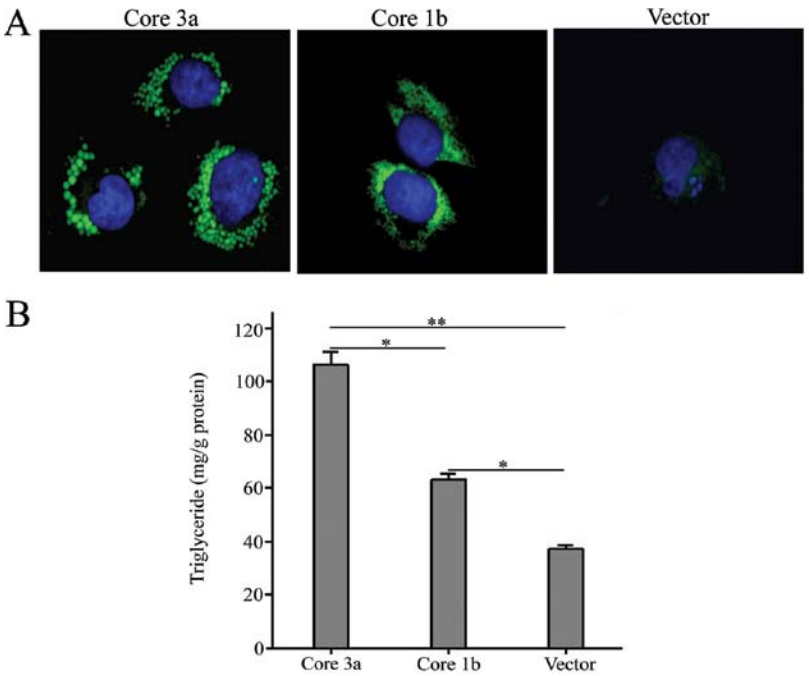

Figure 2. Analyses of the TAG storage and lipid droplets conformation in Huh-7 cells. (A) Lipid droplets conformation in Huh-7 cells. Huh-7 cells were incubated with 100 μM oleic acid overnight to accelerate lipid droplet conformation. Subsequently, cells were fixed and stained with BODIPY 493/503 to observe the lipid droplets by fluorescence microscopy (magnification, x400). The nuclei were stained with Hoechst 33258. (B) Quantification of the cellular TAG in Huh-7 cells. Cellular lipids were extracted and TAG content was tested by a commercial kit. Significant difference between the samples was determined by the Student's t-test (*P<0.05; **P<0.01).

pathways were based on the data from the qRT-PCR result. We first generated a list of all validated target genes to those dysregulated miRNAs (5 miRNAs upregulated and 11 miRNAs downregulated) from an open access platform for the miRNA database miRBase. The result showed a total of 29 and 188 target genes, respectively. Then, a list of all predicted target genes to

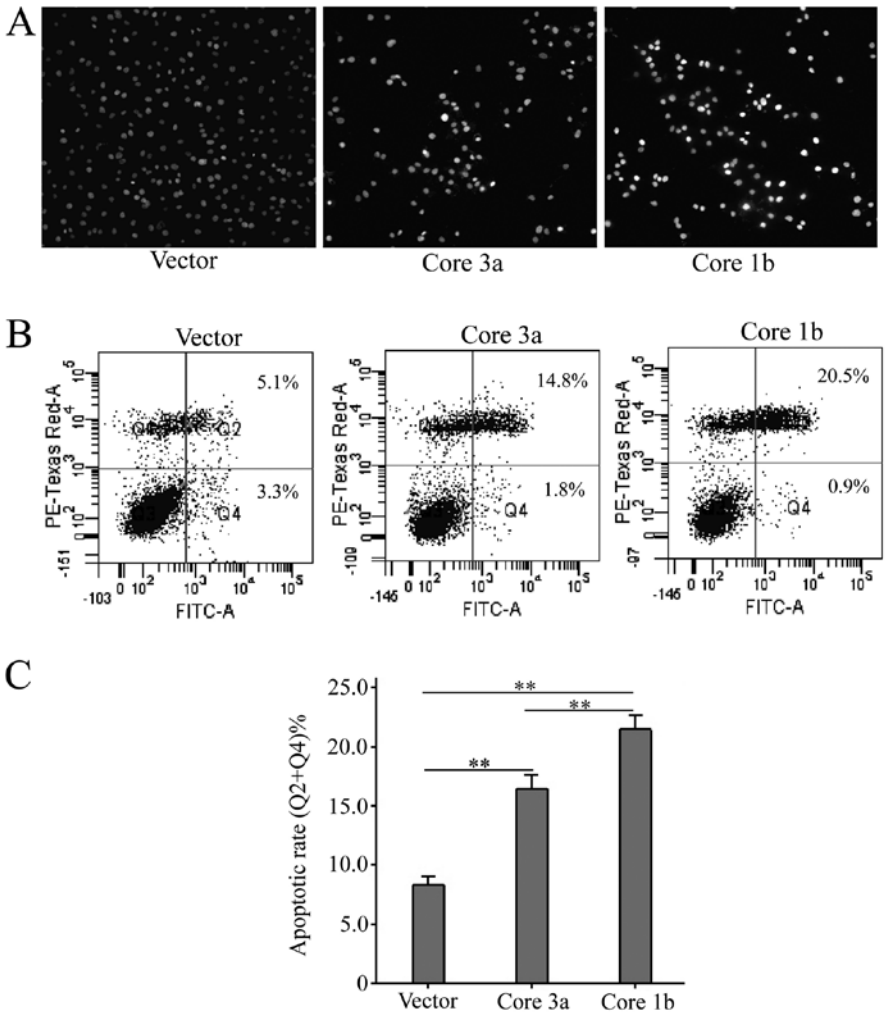

Figure 3. Detection of the apoptosis of Huh-7 cells transfected with HCV core recombinants and blank vector. (A) Changes in nuclear morphology were assessed by Hoechst 33258 staining. (B and C) Apoptosis was determined by FCM of AV/PI staining. Q2 reprents late apoptosis and Q4 reprents early apoptosis. This set of graphs is a representative of three replicates. Statistical significance was determined by the Student's t-test ($^{**}P<0.01$).

those dysregulated miRNAs, including 714 and 1160 genes respectively, was also generated by analyzing the targets from three miRNA target prediction web servers TargetScan, PicTar and the microRNA.org server. Thereafter, a functional annotation and over-representation analysis of the GO biological process (GO BP) terms for those genes were performed using the DAVID program. In this study, a complete list of GO BP terms contained 451 and 495 categories for upregulated and downregulated miRNAs. Table IV lists the top 15 categories of those upregulated and downregulated miRNAs. They mainly include regulation of cellular metabolic processes, regulation of cellular biosynthetic processes, and regulation of gene expression. A similar approach was applied to the enrichment analysis of PANTHER pathway for those genes. A total of 4 and 13 pathways (Table V) were enriched for upregulated and downregulated miRNAs with 3 overlaps, including TGF-β signaling pathway, p53 pathway and integrin signaling pathway.

Confirmation of the functions regulated by HCV core protein and related miRNAs. By GO and PANTHER analyses, dysregulated miRNAs between cells expressing HCV genotype 3a and 1b core are mainly cellular metabolism and apoptosis associated. Several trials were carried out to confirm the functions regulated by HCV core proteins and related miRNAs. Firstly, cellular lipid storage was detected by LDs staining and TAG measuring. As shown in Fig. 2A, the number and size of lipid droplets were increased in cells transfected with HCV core recombinants and cells transfected with genotype 3a had more and larger lipid droplets than those transfected with genotype 1b. Furthermore, TAG measurement was performed. As shown in Fig. 2B, TAG was gradually increased from blank vector to HCV genotype 1b and 3a groups (TAG content, vector, 55.9±1.7; HCV 1b, 94.5±3.6; HCV 3a, 159.5±7.3 μg/mg protein).

Afterwards, cellular apoptosis was assessed by Hoechst 33258 staining and FCM assays. According to the Hoechst 33258 staining of cell nuclei, the percentage of apoptotic cells of the core 1b group was greater than that in the core 3a group, and the lowest in the blank vector group (Fig. 3A). To determine the apoptotic rate of cells accurately, quantitative analysis of apoptosis by FCM of AV/PI dual staining was performed. As shown in Fig. 3B and C, among the blank vector and HCV 3a and 1b groups, the apoptotic rate of cells was gradually increased (apoptotic rate, vector, 8.30±0.36%; HCV 3a, 16.43±0.57%; HCV 1b, 21.47±0.60%). So, HCV core 3a and 1b could affect cellular lipid metabolism and apoptosis differently in Huh-7 cells.

Discussion

Hepatitis C is a world wide contagious liver disease caused by HCV. HCV infection sometimes results in an acute symptomatic illness. However, more than 80% of patients develop a lifelong chronic condition that can lead to steatosis, cirrhosis of the liver and liver cancer (13). In addition, standard antivirus therapy with interferon and ribavirin has resulted in suboptimal responses (14). Thus, it is necessary to study the molecular mechanism of the action of HCV in liver diseases for finding new drug targets. Recently, miRNAs have been demonstrated to play important roles in many physiopathological processes, including HCV infection and hepatitis C. For instance, miR-122 is highly expressed in the liver and plays important roles in cholesterol metabolism, hepatocellular carcinoma and HCV replication (15). IFN-induced miRNAs miR-196 and miR-448 directly target HCV genomic RNA for inhibition of viral replication (16). Thus, it is promising to find additional miRNAs related to HCV infection.

This study was undertaken in order to investigate the effect of HCV core proteins of the two different genotypes 3a and 1b on the miRNA expression profile of Huh-7 cells. Only 7 articles about the relationship between the miRNA expressing profile and HCV infection were retrieved from PubMed and most of the studies have been carried out with genotype 1. HCV is divided into 6 genotypes according to the gene diversity of structure proteins and the clinical and pathogenic data vary among different genotypes. Genotype 1 and 3 are characterized by distinct levels of response to therapy (17,18), severity of liver steatosis (3), insulin resistance (19) and risk of developing cirrhosis and hepatocellular carcinoma (20). Therefore, we were interested in investigating the miRNA expression profiles between genotypes 3a and 1b.

By microarray and real-time PCR assays, a total of 16 miRNAs were determined to be dysregulated (5 miRNAs upregulated and 11 miRNAs downregulated) in Huh-7 cells expressing genotype 3a vs. 1b. Some of these dysregulated miRNAs have been reported to be functional in several pivotal biological processes. miR-423-3p, miR-92b and miR-663 promote cell growth by regulating the G1/S transition (21-23). miR-542-3p, miR-885-5p and miR-192* inhibit cell proliferation and induce cell apoptosis (24-26). miR-224, miR-34b* and miR-95 are associated with the genesis and development of diverse tumors (27-29). miR-192 mediates TGF-β/Smad3 driven renal fibrosis. miR-30 is a key regulator of human adipogenesis (30). The literature indicates that the dysregulated miRNAs have potential functions in steatosis, cirrhosis and liver cancer which are represent the differences in the pathobiology of genotype 3a and 1b. Meanwhile, this simple model of overexpression of core proteins in cell lines is effective in studying the biological function of HCV core protein.

It is known that a miRNA can reduce the levels of many of its target transcripts and function in multiple processes (31). In order to explore the novel functions of the dysregulated miRNAs, their target genes were generated from the miRNA database platform miRBase and then functional categories and biological pathways were analyzed using the free access program DAVID. 704 target genes of 5 upregulated miRNAs and 1298 target genes of 11 downregulated miRNAs were finally determined. By GO analysis, the function categories of both the upregulated and downregulated miRNAs mainly include regulation of cellular metabolic process, biosynthetic process, gene expression and cellular process. Among them, we were interested in the regulation of the cellular metabolic process. As reported, HCV core could play a role in virus-induced steatosis and genotype 3a has stronger effect of lipid droplets induction and FAS activation than genotype 1b (32,33). In this study, we also found some target genes participating in the processes of neutral lipid metabolism and lipid transport. For instance, ACSL1 (target of miR-16-2*), ACSL4 (target of miR-224), and ACSL6 (target of miR-664) are essential for *de novo* lipid synthesis and fatty acid catabolism (34). HMGCR (target of miR-224) catalyzes a rate-limiting step in sterol and isoprenoid biosynthesis (35). FBXW7 (target of miR-92b), INSIG1 (target of miR-92b), and CAV1 (target of miR-34b* and miR-30a*) also play key roles in regulating lipid metabolism and lipid homeostasis in the liver (36-38). ABCA1 (target of miR-885-5p), ABCC1 (target of miR-34b*), and FABP2 (target of miR-132) are tightly associated with the transport of neutral lipid or fatty acids (39,40). CREBBP (target of miR-30a*), RXRA (target of miR-664) and SIRT1 (target of miR-132) are important transcription factors associated with liver lipid metabolism (41,42). Furthermore, we confirmed the difference of core and consequent miRNAs on the effect of lipid storage by carrying out lipid droplets staining and TAG measuring experiments. As shown in Fig. 2, cores of genotype 3a and 1b could induce lipid storage in Huh-7 cells and genotype 3a had a stronger effect, which are consistent with previous studies (9).

As shown in Table V, a total of 13 pathways were identified by PANTHER pathway analysis. In the 3 overlapped pathways, both TGF-β and the p53 pathways are cell growth and apoptosis-associated (43). Additionally, the p53 pathway feedback loops 2, the PI3 kinase pathway (44) and insulin/IGF pathway (45) regulated by downregulated miRNAs, are also related to cell growth, malignant transformation and apoptosis. Therefore, we performed Hoechst 33258 staining and FCM assays to evaluate the cellular apoptosis. Our results showed that core genotypes 3a and 1b could induce apopotosis in Huh-7 cells and genotype 1b had a stronger effect. Until now, the data regarding the role of the HCV core is controversial and has pro- and anti-apoptotic dual effects in death ligand-mediated hepatocyte (46). Admittedly, our experiments about core and apoptosis are short of depth. In any case, HCV core could play important roles in cell growth and apoptosis and some meaningful miRNAs discovered in this study could have some effects.

In conclusion, this study has identified several miRNAs dysregulated by the core proteins of two different HCV genotypes 3a and 1b, generated possible targets of these miRNAs and explored potential downstream GO categories and PANTHER pathways. The results suggest that these miRNAs could function in cellular metabolism and apoptosis, which has been confirmed by some preliminarily assays. However, the pathophysiologic function of an individual miRNA is unclear and more experiments need to be performed in the future. Finally, these miRNAs will contribute to the understanding of the molecular mechanism of liver diseases caused by HCV infection and the search of possible drug targets.

Acknowledgements

We thank members in Qing Li's Laboratory in the Fourth Military Medical University for technical assistance. This study was supported by grants (81000171 and 81170798) from the National Natural Science Foundation of China.

References

1. Khaliq S, Jahan S and Pervaiz A: Sequence variability of HCV core region: important predictors of HCV induced pathogenesis and viral production. Infect Genet Evol 11: 543-556, 2011.
2. Arrese M, Riquelme A and Soza A: Insulin resistance, hepatic steatosis and hepatitis C: a complex relationship with relevant clinical implications. Ann Hepatol (Suppl 9): S112-S118, 2010.
3. Ripoli M and Pazienza V: Impact of HCV genetic differences on pathobiology of disease. Expert Rev Anti Infect Ther 9: 747-759, 2011.
4. Pazienza V, Clement S, Pugnale P, *et al*: Gene expression profile of Huh-7 cells expressing hepatitis C virus genotype 1b or 3a core proteins. Liver Int 29: 661-669, 2009.
5. Wu L and Belasco JG: Let me count the ways: mechanisms of gene regulation by miRNAs and siRNAs. Mol Cell 29: 1-7, 2008.
6. Peng X, Li Y, Walters KA, *et al*: Computational identification of hepatitis C virus associated microRNA-mRNA regulatory modules in human livers. BMC Genomics 10: 373, 2009.
7. Steuerwald NM, Parsons JC, Bennett K, Bates TC and Bonkovsky HL: Parallel microRNA and mRNA expression profiling of (genotype 1b) human hepatoma cells expressing hepatitis C virus. Liver Int 30: 1490-1504, 2010.
8. Jopling CL, Yi M, Lancaster AM, Lemon SM and Sarnow P: Modulation of hepatitis C virus RNA abundance by a liver-specific microRNA. Science 309: 1577-1581, 2005.
9. Abid K, Pazienza V, de Gottardi A, *et al*: An in vitro model of hepatitis C virus genotype 3a-associated triglycerides accumulation. J Hepatol 42: 744-751, 2005.
10. Jin X, Chen YP, Kong M, Zheng L, Yang YD and Li YM: Transition from hepatic steatosis to steatohepatitis: unique microRNA patterns and potential downstream functions and pathways. J Gastroenterol Hepatol 27: 331-340, 2011.
11. Huang da W, Sherman BT, Tan Q, *et al*: DAVID Bioinformatics Resources: expanded annotation database and novel algorithms to better extract biology from large gene lists. Nucleic Acids Res 35: W169-W175, 2007.
12. Folch J, Lees M and Sloane Stanley GH: A simple method for the isolation and purification of total lipides from animal tissues. J Biol Chem 226: 497-509, 1957.
13. Hoofnagle JH: Hepatitis C: the clinical spectrum of disease. Hepatology 26 (Suppl 1): S15-S20, 1997.
14. Klibanov OM, Williams SH, Smith LS, Olin JL and Vickery SB: Telaprevir: a novel NS3/4 protease inhibitor for the treatment of hepatitis C. Pharmacotherapy 31: 951-974, 2011.
15. Jopling C: Liver-specific microRNA-122: Biogenesis and function. RNA Biol 9: 137-142, 2012.
16. Pedersen IM, Cheng G, Wieland S, *et al*: Interferon modulation of cellular microRNAs as an antiviral mechanism. Nature 449: 919-922, 2007.
17. Fried MW, Shiffman M, Sterling RK, *et al*: A multicenter, randomized trial of daily high-dose interferon-alfa 2b for the treatment of chronic hepatitis c: pretreatment stratification by viral burden and genotype. Am J Gastroenterol 95: 3225-3229, 2000.
18. Chevaliez S and Asselah T: Mechanisms of non-response to antiviral treatment in chronic hepatitis C. Clin Res Hepatol Gastroenterol 35 (Suppl 1): S31-S41, 2011.
19. Camma C, Bruno S, Di Marco V, *et al*: Insulin resistance is associated with steatosis in nondiabetic patients with genotype 1 chronic hepatitis C. Hepatology 43: 64-71, 2006.
20. Bruno S, Crosignani A, Maisonneuve P, Rossi S, Silini E and Mondelli MU: Hepatitis C virus genotype 1b as a major risk factor associated with hepatocellular carcinoma in patients with cirrhosis: a seventeen-year prospective cohort study. Hepatology 46: 1350-1356, 2007.
21. Lin J, Huang S, Wu S, *et al*: MicroRNA-423 promotes cell growth and regulates G(1)/S transition by targeting p21Cip1/Waf1 in hepatocellular carcinoma. Carcinogenesis 32: 1641-1647, 2011.
22. Sengupta S, Nie J, Wagner RJ, Yang C, Stewart R and Thomson JA: MicroRNA 92b controls the G1/S checkpoint gene p57 in human embryonic stem cells. Stem Cells 27: 1524-1528, 2009.
23. Yi C, Wang Q, Wang L, *et al*: miR-663, a microRNA targeting p21(WAF1/CIP1), promotes the proliferation and tumorigenesis of nasopharyngeal carcinoma. Oncogene: Jan 16, 2012 (Epub ahead of print).
24. Yoon S, Choi YC, Lee S, Jeong Y, Yoon J and Baek K: Induction of growth arrest by miR-542-3p that targets survivin. FEBS Lett 584: 4048-4052, 2010.
25. Afanasyeva EA, Mestdagh P, Kumps C, *et al*: MicroRNA miR-885-5p targets CDK2 and MCM5, activates p53 and inhibits proliferation and survival. Cell Death Differ 18: 974-984, 2011.
26. Feng S, Cong S, Zhang X, *et al*: MicroRNA-192 targeting retinoblastoma 1 inhibits cell proliferation and induces cell apoptosis in lung cancer cells. Nucleic Acids Res 39: 6669-6678, 2011.
27. Wang Y and Lee CG: Role of miR-224 in hepatocellular carcinoma: a tool for possible therapeutic intervention? Epigenomics 3: 235-243, 2011.
28. Lee YM, Lee JY, Ho CC, *et al*: MicroRNA 34b as a tumor suppressor in estrogen-dependent growth of breast cancer cells. Breast Cancer Res 13: R116, 2011.
29. Huang Z, Huang S, Wang Q, *et al*: MicroRNA-95 promotes cell proliferation and targets sorting Nexin 1 in human colorectal carcinoma. Cancer Res 71: 2582-2589, 2011.
30. Zaragosi LE, Wdziekonski B, Brigand KL, *et al*: Small RNA sequencing reveals miR-642a-3p as a novel adipocyte-specific microRNA and miR-30 as a key regulator of human adipogenesis. Genome Biol 12: R64, 2011.
31. Lim LP, Lau NC, Garrett-Engele P, *et al*: Microarray analysis shows that some microRNAs downregulate large numbers of target mRNAs. Nature 433: 769-773, 2005.
32. Piodi A, Chouteau P, Lerat H, Hezode C and Pawlotsky JM: Morphological changes in intracellular lipid droplets induced by different hepatitis C virus genotype core sequences and relationship with steatosis. Hepatology 48: 16-27, 2008.
33. Jackel-Cram C, Babiuk LA and Liu Q: Up-regulation of fatty acid synthase promoter by hepatitis C virus core protein: genotype-3a core has a stronger effect than genotype-1b core. J Hepatol 46: 999-1008, 2007.
34. Soupene E and Kuypers FA: Mammalian long-chain acyl-CoA synthetases. Exp Biol Med (Maywood) 233: 507-521, 2008.
35. Burg JS and Espenshade PJ: Regulation of HMG-CoA reductase in mammals and yeast. Prog Lipid Res 50: 403-410, 2011.
36. Onoyama I, Suzuki A, Matsumoto A, *et al*: Fbxw7 regulates lipid metabolism and cell fate decisions in the mouse liver. J Clin Invest 121: 342-354, 2010.
37. Loewen CJ and Levine TP: Cholesterol homeostasis: not until the SCAP lady INSIGs. Curr Biol 12: R779-R781, 2002.
38. Martin S and Parton RG: Caveolin, cholesterol, and lipid bodies. Semin Cell Dev Biol 16: 163-174, 2005.
39. Klappe K, Hummel I, Hoekstra D and Kok JW: Lipid dependence of ABC transporter localization and function. Chem Phys Lipids 161: 57-64, 2009.
40. Agellon LB, Drozdowski L, Li L, *et al*: Loss of intestinal fatty acid binding protein increases the susceptibility of male mice to high fat diet-induced fatty liver. Biochim Biophys Acta 1771: 1283-1288, 2007.
41. Schmitt E, Ballou MA, Correa MN, DePeters EJ, Drackley JK and Loor JJ: Dietary lipid during the transition period to manipulate subcutaneous adipose tissue peroxisome proliferator-activated receptor-gamma co-regulator and target gene expression. J Dairy Sci 94: 5913-5925, 2011.
42. Colak Y, Ozturk O, Senates E, *et al*: SIRT1 as a potential therapeutic target for treatment of nonalcoholic fatty liver disease. Med Sci Monit 17: HY5-HY9, 2011.
43. Glasgow E and Mishra L: Transforming growth factor-beta signaling and ubiquitinators in cancer. Endocr Relat Cancer 15: 59-72, 2008.
44. Thorgeirsson SS, Teramoto T and Factor VM: Dysregulation of apoptosis in hepatocellular carcinoma. Semin Liver Dis 18: 115-122, 1998.
45. Breuhahn K and Schirmacher P: Reactivation of the insulin-like growth factor-II signaling pathway in human hepatocellular carcinoma. World J Gastroenterol 14: 1690-1698, 2008.
46. Jahan S, Ashfaq UA, Khaliq S, Samreen B and Afzal N: Dual behavior of HCV core gene in regulation of apoptosis is important in progression of HCC. Infect Genet Evol 12: 236-239, 2012.